The Use of Titanium Dioxide Nanotubes as Photoanodes for Chloride Oxidation

Con Boyle [a], Nathan Skillen [a], H. Q. Nimal Gunaratne [a], Preetam K. Sharma [b], J. Anthony Byrne [b], Peter K.J. Robertson [*a]*

[a] *School of Chemistry and Chemical Engineering, Queen's University Belfast, David Keir Building, Stranmillis Road, Belfast BT9 5AG, United Kingdom*

[b] *Nanotechnology and Integrated BioEngineering Centre, University of Ulster, Shore Road, Newtownabbey, BT37 0QB, United Kingdom*

Abstract

In recent years, significant attention has been given to the development of photoelectrochemical materials capable of producing high current densities under illumination for a range of applications. Titanium dioxide nanotubes (TiNTs) have emerged as a favourable nanomaterial due to a reduced rate of recombination coupled with the ability to generate stable and high photocurrents. To date however, there has been no reports on the use of TiNTs for the photoelectrochemical production of chlorine, a powerful disinfectant, under UV light. The work reported here describes the construction of TiNTs for chlorine generation under low power UV-Light Emitting Diode (UV-LED) irradiation. Linear sweep voltammetry has shown TiNTs to be active for chlorine generation, achieving an average faradaic yield of ~60 %, which was found to be significantly higher when compared to sol-gel electrodes (~40 %). Furthermore, the impact of electrode conditioning was evaluated, demonstrating improved performance after removing surface contaminants.

Keywords; Titanium Dioxide Nanotubes, Chlorine, Photoelectrochemistry, UV Irradiation

1. Introduction

The initial publication by Fujishima and Honda in 1972 demonstrated the capability of both TiO_2 and photoelectrochemistry (PEC) to be utilised for water splitting [1]. Since then, material development for photocatalytic and PEC systems has grown significantly with published articles now covering a diverse range of compounds and applications [2]–[4]. While there are a range of materials deployed by researchers for PEC application, titania based materials remain one of the most commonly reported with a key focus being to improve the overall efficiency and activity [5]. Regardless of the application, photocatalytic material activity is generally dictated by their ability to absorb light and to generate and allow sufficient migration of the electron-hole pairs to facilitate a desired chemical reaction. These key properties are largely influenced by physical, chemical and electronic properties such as surface area, crystal phase and geometry [6]. As a result, research has focused on the development of nanostructured catalysts such as nanotubes [7], nanowires [8] and nanorods [9], with a view towards increasing photocatalytic activity.

Titania nanotubes (TiNTs) have been reported in the literature for use in both photocatalytic and PEC applications [10]. In PEC systems, TiNTs are known to exhibit increased light penetration and absorption allowing for the generation of higher photocurrents under lower irradiance. The formation of TiNTs can be achieved *via* template assisted [11], hydrothermal [12], [13], and anodic oxidation [14], [15] methods. Anodic oxidation in the presence of fluoride ions is an attractive and consistent method of nanotube formation, providing uniform self-ordered nanotubes [7], with easy control of the length and diameter of the nanotubes *via* control over the applied voltage and duration [10].

There are numerous examples of TiNTs being deployed for a range of applications including air purification [16], *E-coli* degradation [17] and water splitting for hydrogen production [18]–[20]. A less frequently reported application for TiO_2 PEC systems, however, is the oxidation of chloride to chlorine. While chlorine plays a pivotal role as a disinfectant in water treatment and in polyvinylchloride (PVC) production, it is primarily formed *via* an energy intensive electrochemical process in the chlor-alkali industry [21]. Therefore, the generation of chlorine *via* photocatalytic or PEC routes under low energy conditions represents a more efficient and favourable approach. To date, however, there has been limited examples reported in the literature which have achieved this. Anderson *et al.* demonstrated the production of chlorine on nanocrystalline TiO_2 thin-film electrodes [22], and subsequent work by Fraga *et al.* evaluated the PEC formation of active chlorine with simultaneous removal of microcystin toxins [23]. Chlorine/hypochlorite formation was also demonstrated on "roll-on" nanostructured WO_3 films annealed on indium tin oxide (ITO) substrates by Ahmed *et al.* [24].

Therefore, presented in this work is the use of TiNTs for chloride oxidation to chlorine under irradiation from a single low power UV-Light Emitting Diode (UV-LED). This is the first report of TiNTs being deployed for this application under UV-LED irradiation. Linear sweep voltammetry was performed on TiNTs for both chloride and water

oxidation along with chlorine yield analysis with average faradaic efficiencies of 60.6 % on TiNTs for chlorine generation being achieved. Furthermore, the performance of TiNTs was compared to that of TiO_2 sol-gel electrodes, with the former exhibiting higher photoelectrochemical activity.

2. Experimental

2.1 Anodization

Titanium coupons (25 x 25 mm) with a thickness of 0.1 mm and a purity of 99.6 % were purchased from Goodfellow chemicals. The titanium coupons were degreased in methanol by sonication for 15 min, rinsed with de-ionised water and dried in air. Once dry, the titanium was placed in a 150 mL beaker containing electrolyte and a platinum counter electrode. The electrolyte was 0.3 wt % ammonium fluoride dissolved in 97 vol% ethylene glycol and 3 vol% distilled water. Electrical connections were made to both the anode and cathode by means of crocodile clips attached to areas which were not in contact with the solution. The counter electrode was held in parallel at 3 cm away from the anode. Anodization was carried out at 30 V for 3 hrs and once completed the anodized titania was rinsed in de-ionised water and placed in a furnace at 450°C for 30 min.

The morphology of the nanotubes was determined using a Hitachi SU5000 field emission scanning electron microscope (FESEM) operated at 5 kV. The energy dispersive X-ray measurements were performed using the Oxford Instruments X-Max^N detector coupled with the Hitachi electron microscope (FESEM-EDX) at 10 kV electron acceleration. X-ray diffraction (XRD) analysis was carried out using a PANanalytical X'Pert Pro X-ray diffractometer in 20 - 60 degrees 2θ range. Furthermore, BET analysis was carried out on a Tristar II 3020 (Micromeretics), capable of measuring specific surface areas from 0.01 m^2 g^{-1}. The analysis utilised nitrogen gas adsorption at 77.35 K from 0 – 0.995 P/P_0.

2.2 Sol-gel electrodes

Titanium coupons (25 x 25 mm) were first etched in 18 % hydrochloric acid and 10 % by weight oxalic acid. The solution was heated to 95 °C and stirred, with the coupons being soaked in the solution for around 30 minutes to ensure a uniform etching process, then rinsed with de-ionised water and stored in methanol. TiO_2 was made using the sol-gel process as described by Mills *et al.* [25]. In brief, 4.65 g of glacial acetic acid was added to 20 mL of titanium isopropoxide (Sigma Aldrich) and then mixed with 120 mL of water and 1.08 g of concentrated nitric acid. This solution was constantly stirred and heated to 80°C for 8 hr. Once cooled, the solution was filtered using a 0.45 µM filter and transferred into a Teflon™ pot which was then placed in an autoclave for 12 hr at 220°C. Finally, the TiO_2 sol-gel was placed in a rotary evaporator to concentrate the solution to approx. 10-12 wt% TiO_2 (anatase). The sol-gel was then

applied to the etched coupons using the doctor blade technique [25], where Scotch Magic Tape™ was used to hold the etched coupons in place and create a template area for the coating. A glass rod was then used to "draw" the applied sol-gel across the electrode and form an even coating. Once an even coating was achieved, the TiO_2 was allowed to dry in air for 1 hr and then placed in a furnace at 450°C for 30 min.

2.3 PEC studies

Experiments were carried out in a 3-electrode modified photoelectrochemical cell as described by Tang-Kong *et al.* [21], where an Ag/AgCl reference electrode was employed and the counter electrode was a 1 mm diameter platinum wire (
Figure 1). Experiments were carried out in 10 mL of 0.5 M H_2SO_4, and acid/chloride experiments in 10 mL of 0.5M H_2SO_4 containing 3.5 M NaCl (SciChem). The electrolyte was purged for 10 minutes with argon before any photoelectrochemical measurements were initiated to remove any dissolved gas. The photoanode was placed underneath the PTFE cell and electrical contact from the potentiostat (Ivium technologies) was made through use of a titanium strip and crocodile clip. The PTFE cell was then clamped down on top of the working electrode to ensure an air tight seal and leave an exposed geometric surface area of 0.196 cm^2. A 1 W UV-A LED (LED Engin), with a V_F = 3.5 dcV and I_F = 0.25 A was positioned above the PTFE cell and UV light reached the photoanode through a quartz glass window (Newcastle optical). Irradiance of the light source was measured using a UV-X radiometer.

Linear sweep voltammetry (LSV) was typically carried out in both dark and illuminated conditions from -0.1 V to +1.0 V at a scan rate of 1 mV/s firstly in 0.5 M H_2SO_4 for water oxidation. The electrolyte was then replaced with 3.5 M NaCl dissolved in 0.5 M H_2SO_4 for chloride oxidation. For chlorine faradaic yield analysis, chronoamperometry was used to apply a constant potential to the irradiated photoanode for 1 hr. Argon gas was used to purge generated chlorine from the system (for 1 hr after chronoamperometry) and into a trap solution [26], containing potassium iodide (0.36 M), sodium hydroxide (0.025 M) and potassium hydrogen phthalate (0.049 M) which turned yellow upon exposure to chlorine due to the formation of tri-iodide (I^{3-}). A 1.5 mL sample was then taken, and the absorbance was measured at 353 nm in a Cary 300 UV/Vis spectrophotometer. Using the Beer-Lambert law the concentration of chlorine formed can be deduced allowing for yield calculations against the theoretical concentrations formed.

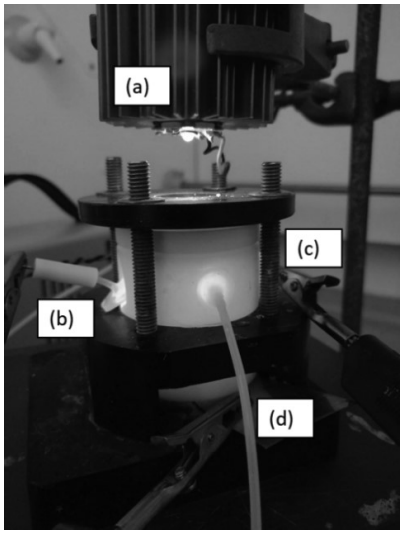

Figure 1; Photo of the PEC system used to analyse TiNTs under UV illumination. A 1 W UV LED (a), an Ag/AgCl reference electrode (b), a platinum counter (c) were employed. A titanium strip was used to connect the TiO_2 working electrode *via* crocodile clip (d).

3. Results and Discussion

3.1 Nanotube formation

The formation of TiO_2 nanotubes can be impacted by several factors including electrolyte, applied voltage and surface roughness [14]. It is important that for photocatalytic coatings such as TiNTs that there is large coverage of the TiO_2 material across the surface morphology and that nanotube formation is uniform. Figure 2(a) shows a top down SEM image of the self-organised nanotubes formed on the surface of the titanium coupons, highlighting excellent coverage and uniformity across the film. The nanotubes had an average diameter of, ~ 97.1 nm, with an average inner diameter of ~74.56 nm. Figure 2(b) shows a top down SEM image of the TiO_2 sol-gel nanoparticles. Furthermore, XRD analysis confirmed the crystal phase of the TiO_2 formed by the anodization and sol-gel processes to be anatase (Figure S1).

(a) (b)

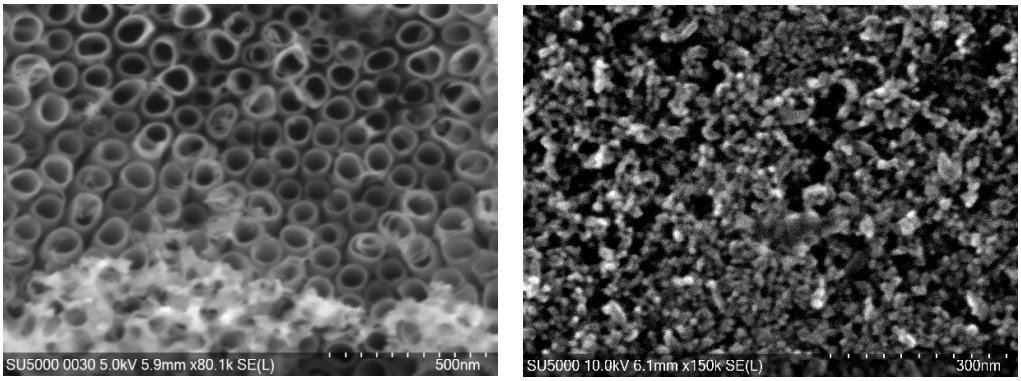

Figure 2; (a) SEM image of the titania nanotubes formed during the anodization process, showing tubular formation and large surface coverage (b) SEM image of the sol-gel nanoparticles.

3.2 Linear Sweep Voltammetry

Linear sweep voltammetry (LSV) was conducted with the nanotubes to assess their performance for the generation of oxygen and chlorine. The photocurrents generated for water and chloride oxidation under UV illumination (7.08 mW cm^{-2}) are shown in Figure 3 (a). As can be seen, the observed photocurrent between 0 – 0.5 V was higher for chlorine generation than oxygen. TiNTs have previously been used for water splitting applications to produce hydrogen and oxygen with photocurrent densities as high as 1.59 mA cm^{-2} reported amongst literature [18]. Interestingly, photocurrent densities as high as 1.02 mA cm^{-2} at a potential of +1.0 V have been achieved here for oxygen evolution under a low irradiance (7.08 mW cm^{-2}) from an energy efficient LED. More significantly however, the LSV data also shows that chlorine generation can take place on TiNTs at potentials such as 0.2 V (Ag/AgCl), which is much lower than the standard electrochemical redox potential for chloride oxidation at 1.36 eV (vs NHE) [27], highlighting the benefit of PEC systems.

Sol-gel TiO_2 is a commonly used material for photocatalytic applications and has previously been demonstrated for use in PEC applications [28]. Therefore, further testing was also carried out on sol-gel electrodes for the application of chloride oxidation and their performance compared against that of the TiNTs. The TiNTs outperformed the sol-gel TiO_2 in terms of photocurrent density produced under UV illumination (Figure 3(b)). Furthermore, the onset potential required for chlorine production on the sol-gel films was higher (~ +0.4 V) than that of the nanotubes (0 – 0.2 V). BET analysis showed sol-gel TiO_2 nanoparticles to have approximately ten times higher surface area (0.399 m^2 g^{-1}) than that of TiNTs (0.0397 m^2 g^{-1}) which agrees with literature trends [25], [29]. The values reported here are much smaller due to the BET being carried out as a thin film loaded on Ti coupons as opposed to powdered form. Despite the difference in surface area, it is factors such as morphology and increased light penetration which result in the generation of much higher photocurrent densities on TiNTs. Nanotubes also have less grain boundaries than nanoparticle coatings, thereby exhibiting a lower rate of charge trapping and

recombination [29], resulting in chloride oxidation being more thermodynamically favourable on TiNTs at lower potentials.

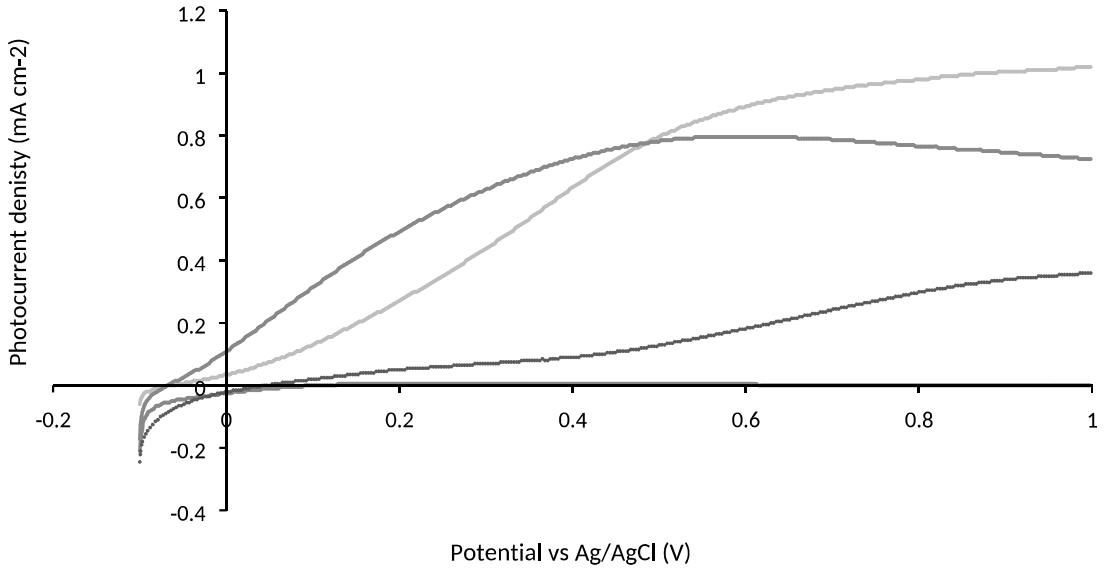

Figure 3; LSV (scan rate 1 mV s^{-1}) carried out for water oxidation (□ ● ●) (0.5 M H_2SO_4) and chloride oxidation (□ □ □) (3.5 M NaCl in 0.5 M H_2SO_4) on TiNTs and for dark control conditions (no UV illumination) (□). Also shown is a LSV carried out for chloride oxidation on sol-gel photoelectrodes (····).

3.3 Chlorine Yields and Electrode Conditioning

To draw a more accurate comparison between the performance of two types of electrode it is important to assess the associated faradaic efficiency (yields). Chronoamperometry was performed on the electrodes and argon was used to purge any chlorine formed into the trap solution. For TiNTs analysis, a typical irradiance on the catalyst surface of 7.08 mW cm^{-2} was used with an applied voltage of +0.2 V, with yield experiments typically carried out in a sequential (back to back) nature. Interestingly, the first experimental run carried out typically yielded a lower value than those that followed which suggests a conditioning step on the electrode was required. Figure 4 shows while the initial faradaic yields achieved at various applied voltages were all < 14 %, a significant increase was obtained on the subsequent experimental runs with yields reaching 28 – 52 %. At +0.2 V the faradaic yield increased from 13.6 to 52.3 % as a result of conditioning, highlighting the importance of this procedure for achieving maximum performance from the electrodes. A similar trend was observed when using sol-gel electrodes. (Figure S2)

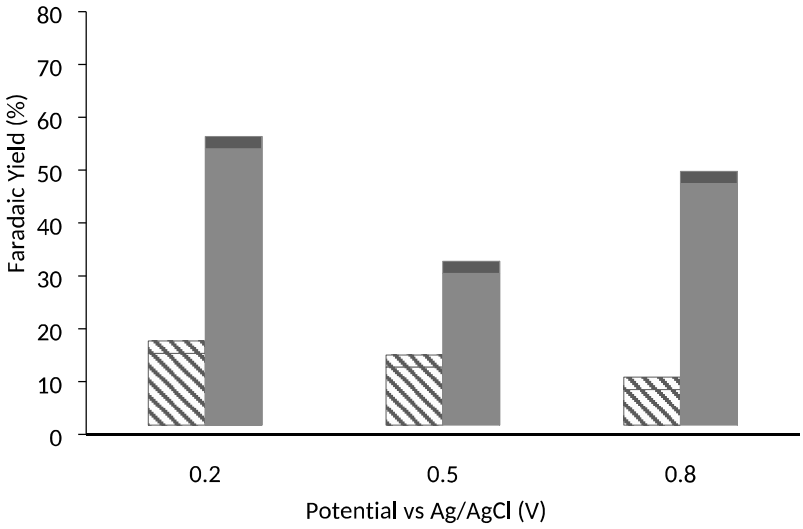

Figure 4; Graph showing example faradaic yields for chloride oxidation on TiNTs at three varied applied potentials (+0.2, +0.5 and +0.8 V) with the 1st yield carried out seen as a conditioning step (▨) and a subsequent yield carried out after conditioning (■).

The conditioning step was likely required due to the presence of unwanted contaminants on the surface of the electrode, which were readily oxidised by chlorine formed. While this has been suggested previously in literature [21], it is yet to be fully investigated. Figure 5 shows the results of EDX carried out on the anodized electrodes before and after photoelectrochemical chloride oxidation. Despite annealing the TiNTs at 450 °C, carbon was still present (Figure 5), which was likely from the electrolyte used during anodization. While it was expected that the annealing step would remove any organics present including carbon, it was found that only after the PEC unit was operated for chlorine generation that a large reduction in carbon was observed. Following PEC operation, EDX revealed the main composition of the material to be titanium and oxygen. The mechanism for carbon removal is not fully understood but may be a synergistic effect from oxidation by photocatalysis and chlorine species formed under UV.

The EDX results shown further back up that of the yield data, which suggests the need for a conditioning step on the electrodes before maximum performance can be reached. Unwanted contaminants which find their way onto the electrode or electrochemical cell between experiments may be oxidised by chlorine formed during the PEC process. Therefore, chlorine formed is not purged from the system into the trap solution for analysis thereby hindering the results as suggested previously [21]. The typical increase in secondary yields suggests the removal of contaminants allowing for more accurate analysis.

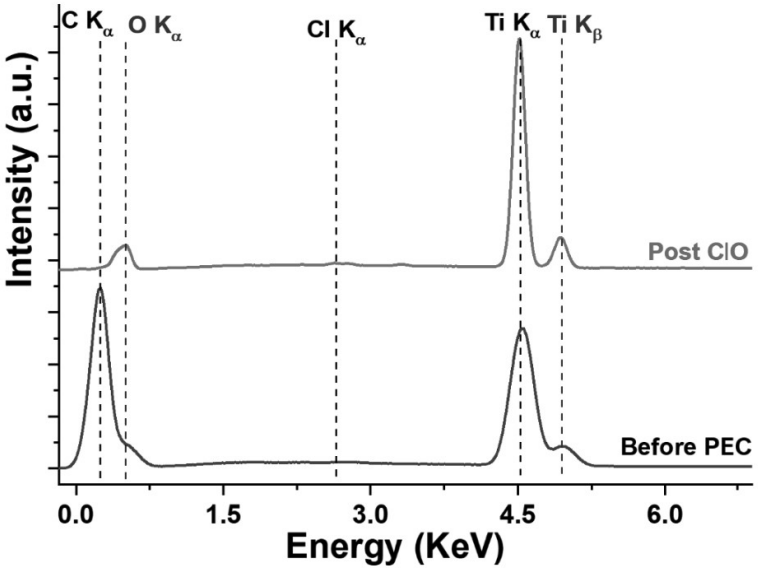

Figure 5; EDX spectra of annealed nanotubes before and after chloride oxidation.

Further yield tests were subsequently carried out to assess the faradaic efficiency of both sol-gel and TiNTs for chlorine generation after the conditioning step. It is important to note that to generate higher photocurrents on sol-gel electrodes at +1.0 V a higher LED irradiance, 16.09 mW cm^{-2}, from the same light source was used during chronoamperometry. In comparison the irradiance used on nanotubes during chronoamperometry at an applied potential of +0.2 V was kept at 7.08 mW cm^{-2}. This was done to keep the charge generated by each electrode as similar as possible during the 1 hr chronoamperometry (see ESI for an example chronoamperogram)

Repeated experimental cycles conducted on the conditioned electrodes highlighted the increase in yields when using TiNTs over the sol-gel material (Table 1 and Figure 6). Figure 6 shows the average yields along with four experimental repeats (post-conditioning) for both sol-gel electrode and TiNTs. An average faradaic yield of ~60 % was obtained for TiNTs operated at +0.2 V and an irradiance of 7.08 mW cm^{-2}. In contrast, at a higher applied potential and higher irradiance, the sol-gel material achieved a faradaic yield of only ~40 % (Table 1). These results suggest that the TiNTs have a higher selectivity to chloride oxidation than that of sol-gel electrodes, with the oxidation of water being an unavoidable side reaction within anodic oxidation processes [22] reducing the efficiency of photoanode materials. The higher faradaic

efficiency associated with TiNTs is likely due to the separation between the chloride and water oxidation LSVs at the applied potential of +0.2 V as shown in Figure 3.

These results demonstrate the benefit of TiNTs for PEC applications and for chlorine generation. The TiNTs produced higher concentrations of chlorine and exhibited higher efficiency at lower applied potentials and under lower irradiance.

Electrode	Irradiance (mW cm^{-2})	Applied potential vs Ag/AgCl (V)	Average Faradaic Efficiency
TiNTs	7.08	+ 0.2	60.61
Sol-gel	16.09	+ 1.0	39.12

Table 1; Chronoamperometry operating parameters for both TiNTs and sol-gel electrodes and associated average faradaic efficiency

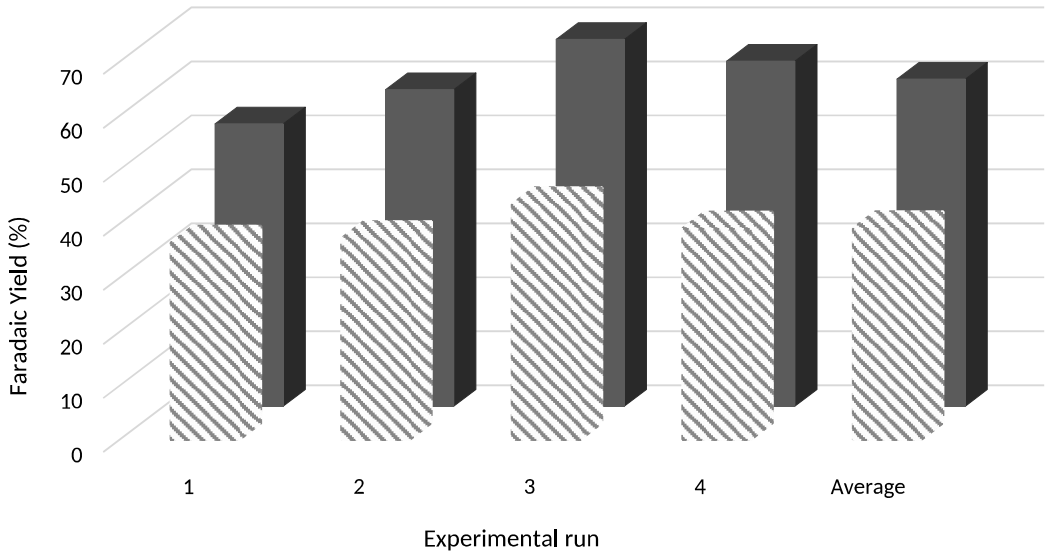

Figure 6; Graph showing the faradaic yields (post-conditioning) for chlorine generation on both sol-gel (▨) (+1.0 V applied potential) and TiNTs (■) (+0.2 V applied potential) with repeats and average values shown.

4. Conclusions

TiNTs have been demonstrated as a capable material to produce chlorine from sodium chloride at low onset potentials under UV illumination. They have also been shown to outperform that of sol-gel electrodes. The sol-gel has also been shown as a capable material for chloride oxidation with faradaic efficiencies of ~40 % but the nanostructured titania exhibits higher photocurrents and higher faradaic efficiencies (60.6 %) at lower potentials and under lower UV irradiation (7.08 mW cm^{-2}) showing great potential for this and other photoelectrochemical applications. Furthermore, the significance of electrode conditioning has been demonstrated with the efficiency of chlorine generation increasing by as much as 20 – 40% post conditioning.

Acknowledgments

The authors wish to acknowledge the financial support of Northern Irelands Department of Economy for the funding of Con Boyle's PhD and Queen's University Belfast Energy Pioneering Research Programme (PRP) for funding the research of Dr. Nathan Skillen. We would also like to thank AVX Ltd and Invest Northern Ireland for financial assistance.

References

[1] A. Fujishima and K. Honda, "Electrochemical photolysis of water at a semiconductor electrode," *Nature*, vol. 238, no. 5358, pp. 37–38, 1972.

[2] J. C. Ireland, P. Klostermann, E. W. Rice, and R. M. Clark, "Inactivation of Escherichia coli by titanium dioxide photocatalytic oxidation.," *Appl. Envir. Microbiol.*, vol. 59, no. 5, pp. 1668–1670, 1993.

[3] P. K. J. Robertson, J. M. C. Robertson, and D. W. Bahnemann, "Removal of microorganisms and their chemical metabolites from water using semiconductor photocatalysis," *J. Hazard. Mater.*, vol. 211–212, pp. 161–171, 2012.

[4] S. Nagarajan, N. C. Skillen, J. T. S. Irvine, L. A. Lawton, and P. K. J. Robertson, "Cellulose II as bioethanol feedstock and its advantages over native cellulose," *Renew. Sustain. Energy Rev.*, vol. 77, no. April, pp. 182–192, 2017.

[5] K. Maeda, "Photocatalytic water splitting using semiconductor particles: History and recent developments," *J. Photochem. Photobiol. C Photochem. Rev.*, vol. 12, no. 4, pp. 237–268, 2011.

[6] M. R. Hoffmann, S. T. Martin, W. Choi, and D. W. Bahnemann, "Environmental Applications of Semiconductor Photocatalysis," *Chem. Rev.*, vol. 95, no. 1, pp. 69–96, 1995.

[7] Y. Zhao, N. Hoivik, and K. Wang, "Recent advance on engineering titanium dioxide nanotubes for photochemical and photoelectrochemical water splitting," *Nano Energy*, vol. 30, pp. 728–744, 2016.

[8] J. Jitputti, Y. Suzuki, and S. Yoshikawa, "Synthesis of TiO2 nanowires and their photocatalytic activity for hydrogen evolution," *Catal. Commun.*, vol. 9, no. 6, pp.

1265–1271, 2008.

[9] A. Wolcott, W. A. Smith, T. R. Kuykendall, Y. Zhao, and J. Z. Zhang, “Photoelectrochemical water splitting using dense and aligned TiO 2 nanorod arrays,” *Small*, vol. 5, no. 1, pp. 104–111, 2009.

[10] M. Abdullah and S. K. Kamarudin, “Titanium dioxide nanotubes (TNT) in energy and environmental applications: An overview,” *Renew. Sustain. Energy Rev.*, vol. 76, no. February 2016, pp. 212–225, 2017.

[11] M. Karaman, F. Sariipek, Ö. Köysüren, and H. B. Yildiz, “Template assisted synthesis of photocatalytic titanium dioxide nanotubes by hot filament chemical vapor deposition method,” *Appl. Surf. Sci.*, vol. 283, pp. 993–998, 2013.

[12] T. Kasuga, M. Hiramatsu, A. Hoson, T. Sekino, and K. Niihara, “Formation of Titanium Oxide Nanotube,” *Langmuir*, vol. 14, no. 12, pp. 3160–3163, 1998.

[13] R. Camposeco, S. Castillo, I. Mejia-Centeno, J. Navarrete, and R. Gómez, “Effect of the Ti/Na molar ratio on the acidity and the structure of TiO2 nanostructures: Nanotubes, nanofibers and nanowires,” *Mater. Charact.*, vol. 90, pp. 113–120, 2014.

[14] G. R. Dale, J. W. J. Hamilton, P. S. M. Dunlop, P. Lemoine, and J. A. Byrne, “Electrochemical Growth of Titanium Oxide Nanotubes : The Effect of Surface Roughness and Applied Potential,” vol. 9, no. xx, pp. 1–5, 2009.

[15] O. Robinson Aguirre and E. Félix Echeverría, “Effects of fluoride source on the characteristics of titanium dioxide nanotubes,” *Appl. Surf. Sci.*, vol. 445, pp. 308–319, 2018.

[16] H. Sopha *et al.*, “Scaling up anodic TiO 2 nanotube layers for gas phase photocatalysis,” *Electrochem. commun.*, vol. 97, no. October, pp. 91–95, 2018.

[17] C. Pablos *et al.*, “Electrochemical Enhancement of Photocatalytic Disinfection on Aligned TiO2 and Nitrogen Doped TiO2 Nanotubes,” *Molecules*, vol. 22, no. 5, p. 704, 2017.

[18] Z. Zhang and P. Wang, “Optimization of photoelectrochemical water splitting performance on hierarchical TiO<inf>2</inf> nanotube arrays,” *Energy Environ. Sci.*, vol. 5, no. 4, pp. 6506–6512, 2012.

[19] Y. Sun, G. Wang, and K. Yan, “TiO2 nanotubes for hydrogen generation by photocatalytic water splitting in a two-compartment photoelectrochemical cell,” *Int. J. Hydrogen Energy*, vol. 36, no. 24, pp. 15502–15508, 2011.

[20] Z. Zhang, M. F. Hossain, and T. Takahashi, “Photoelectrochemical water splitting on highly smooth and ordered TiO 2 nanotube arrays for hydrogen generation,” *Int. J. Hydrogen Energy*, vol. 35, no. 16, pp. 8528–8535, 2010.

[21] R. Tang-Kong, C. O’Rourke, A. Mills, and P. C. McIntyre, “Silicon Photoanodes for Solar-Driven Oxidation of Brine: A Nanoscale, Photo-Active Analog of the Dimensionally-Stable Anode,” *J. Electrochem. Soc.*, vol. 165, no. 16, pp. H1072–H1079, 2018.

[22] M. V. B. Zanoni, J. J. Sene, H. Selcuk, and M. A. Anderson, “Photoelectrocatalytic production of active chlorine on nanocrystalline titanium

dioxide thin-film electrodes," *Environ. Sci. Technol.*, vol. 38, no. 11, pp. 3203–3208, 2004.

[23] L. E. Fraga, M. A. Anderson, M. L. P. M. A. Beatriz, F. M. M. Paschoal, L. P. Romão, and M. V. B. Zanoni, "Evaluation of the photoelectrocatalytic method for oxidizing chloride and simultaneous removal of microcystin toxins in surface waters," *Electrochim. Acta*, vol. 54, no. 7, pp. 2069–2076, 2009.

[24] S. Ahmed, I. A. I. Hassan, H. Roy, and F. Marken, "Photoelectrochemical Transients for Chlorine / Hypochlorite Formation at ' Roll-On ' Nano-WO 3 Film Electrodes," *J. Phys. Chem. C*, 2013.

[25] A. Mills, N. Elliott, G. Hill, D. Fallis, J. R. Durrant, and R. L. Willis, "Preparation and characterisation of novel thick sol–gel titania film photocatalysts," *Photochem. Photobiol. Sci.*, vol. 2, no. 5, pp. 591–596, 2003.

[26] A. Mills and A. Cook, "Analysis of Chlorine = Oxygen Gas Mixtures," vol. 112, no. September, pp. 99–101, 1987.

[27] A. Mills and D. Worsley, "Oxidation of chloride to chlorine by Ce^{IV} ions mediated by different Ru^{IV} and Ir^{IV} oxide-based catalysts," *J. Chem. Soc. Faraday Trans.*, vol. 87, no. 19, pp. 3275–3284, 1991.

[28] Y. Xu, Y. He, X. Cao, D. Zhong, and J. Jia, "TiO2/Ti rotating disk photoelectrocatalytic (PEC) reactor: A combination of highly effective thin-film PEC and conventional PEC processes on a single electrode," *Environ. Sci. Technol.*, vol. 42, no. 7, pp. 2612–2617, 2008.

[29] G. R. Dale, J. W. J. Hamilton, P. S. M. Dunlop, and J. A. Byrne, "Electrochemically assisted photocatalysis on anodic titania nanotubes," vol. 1, 2006.

Supplementary Information

The Use of Titanium Dioxide Nanotubes as Photoanodes for Chloride Oxidation

*Con Boyle [a], Nathan Skillen [a], H. Q. Nimal Gunaratne [a], Preetam K. Sharma [b], J. Anthony Byrne [b], Peter K.J. Robertson *[a]*

[a] *School of Chemistry and Chemical Engineering, Queen's University Belfast, David Keir Building, Stranmillis Road, Belfast BT9 5AG, United Kingdom*

[b] *Nanotechnology and Integrated BioEngineering Centre, University of Ulster, Shore Road, Newtownabbey, BT37 0QB, United Kingdom*

Figure S1 shows XRD for TiNTs compared with a sample of standard TiO_2 anatase (PC500) and a blank titanium coupon as purchased from Goodfellow. The peaks show the TiNTs to match the crystal phase of anatase after the annealing step with key anatase peaks present at ~ 25 and ~ 48 2θ matching that of the standard anatase sample. XRD of the sol-gel TiO2 is also shown to be completely anatase.

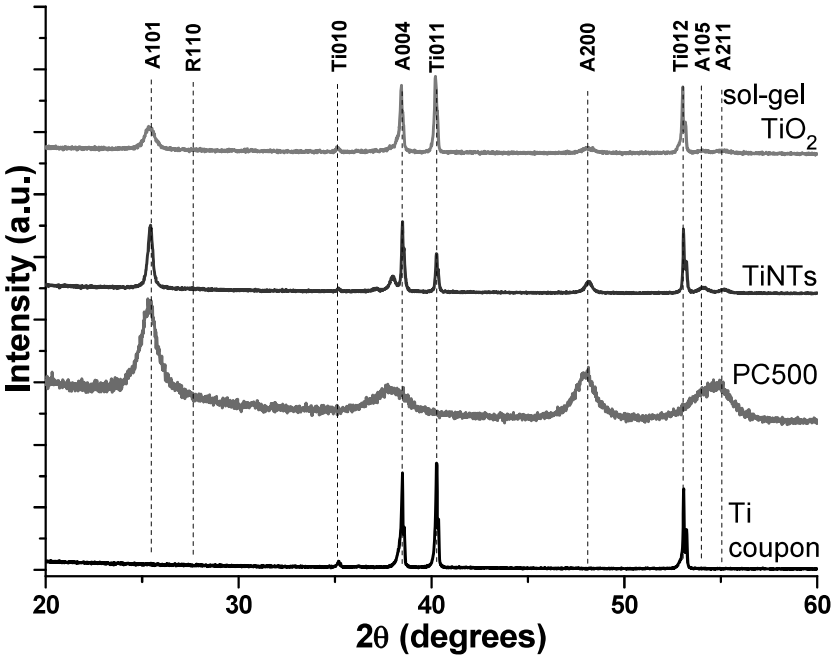

Figure S1; XRD analysis of TiNTs (□) compared with that of anatase TiO_2 (PC 500) (□) and an as purchased titanium coupon from Goodfellow chemicals (□). Also shown is XRD of a sol-gel TiO2 sample (□).

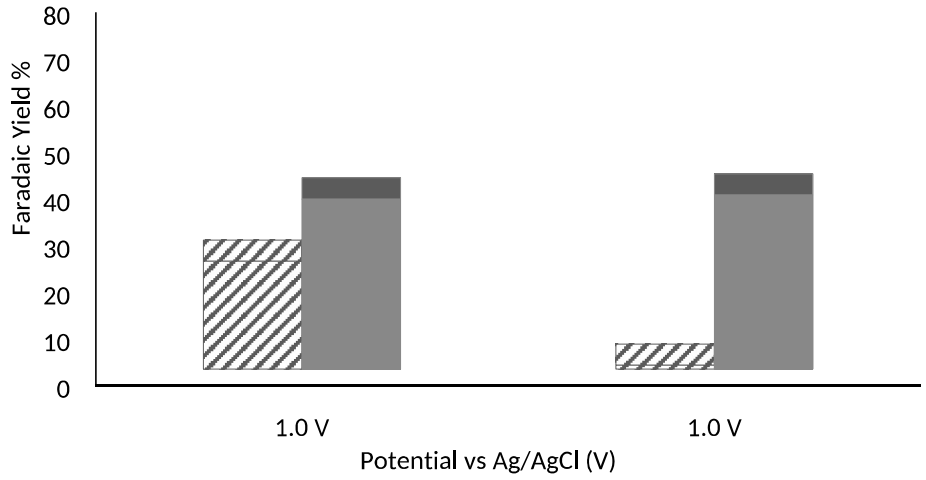

Figure S2; Graph showing example faradaic yields for chloride oxidation on sol-gel electrodes at +1.0 V and with a repeat on the same electrode shown. The 1st yield carried out seen as a conditioning step (▨) and a subsequent yield carried out after conditioning (■).

Figure S3 shows a typical chronoamperogram and the photocurrent generated during UV illumination at an applied voltage of +0.2 V (vs Ag/AgCl). Variation and noise on the graph shown was due to light scattering through bubbles generated by the argon purge gas during the reaction. The graph shown led to a total charge of 0.1649 A s used to calculate the theoretical concentration of chlorine formed during the reaction.

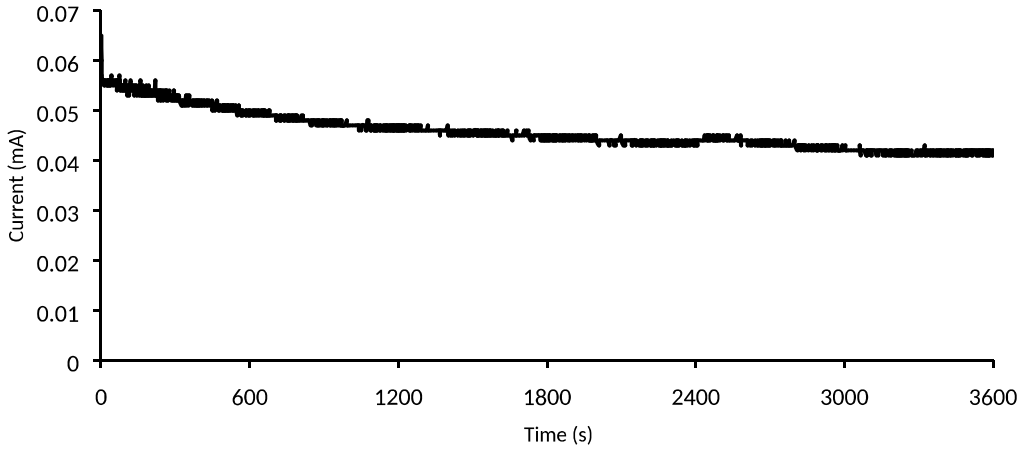

Figure S3; Example chronoamperogram for chloride oxidation on TiNTs- under UV illumination at an applied potential of +0.2 V (vs Ag/AgCl).

* Corresponding author. Tel.: +44 (0)28 9097 4627; E-mail address: p.robertson@qub.ac.uk

The Use of Titanium Dioxide Nanotubes as Photoanodes for Chloride Oxidation

Con Boyle, Nathan Skillen, H. Q. Nimal Gunaratne, Preetam K. Sharma, J. Anthony Byrne, Peter K.J. Robertson.

Declaration of interest statement.

The authors wish to state that the organisations involved in funding the research have been detailed in the acknowledgement sections as follows:

“The authors wish to acknowledge the financial support of Northern Irelands Department of Economy for the funding of Con Boyle’s PhD and Queen’s University Belfast Energy Pioneering Research Programme (PRP) for funding the research of Dr. Nathan Skillen. We would also like to thank AVX Ltd and Invest Northern Ireland for financial assistance.”

No other interests are declared.

The Use of Titanium Dioxide Nanotubes as Photoanodes for Chloride Oxidation

Con Boyle, Nathan Skillen, H. Q. Nimal Gunaratne, Preetam K. Sharma, J. Anthony Byrne, Peter K.J. Robertson.

Author Statement.

The contribution of the authors is as follows:

Con Boyle – Carried out experimental work and prepared original draft of manuscript

Nathan Skillen – involved in developing experimental and reactor design and preparation of manuscript

H. Q. Nimal Gunaratne –Involved in supervision of Con Boyle, advised on experimental design and preparing manuscript

Preetam K. Sharma – involved in preparing anodised films and surface analysis work using SEM and EDX and provided input to preparation of manuscript

J. Anthony Byrne, - advised on preparation of anodised films and on manuscript draft

Peter K.J. Robertson – Principal investigator of overall project, supervisor of Con Boyle's PhD studentship also involved in preparation of final manuscript